NRL REPORT N-3463

FR3463

PASSIVE BEARING FINDER REPORT NO 1

EFFECT OF SYNCHRONIZED TIME-GATING ON THE SIGNAL-TO-NOISE RATIO OF A BROADBAND AMPLIFIER

NAVAL RESEARCH LABORATORY

WASHINGTON, D.C.

NRL REPORT N-3463

PASSIVE BEARING FINDER REPORT NO 1

EFFECT OF SYNCHRONIZED TIME-GATING ON THE SIGNAL-TO-NOISE RATIO OF A BROADBAND AMPLIFIER

J. W. Tucker

September 15, 1949

Approved by:

H. L. Clark, Head, Applied Optics Branch
J. A. Sanderson, Superintendent (Acting), Optics Division

NAVAL RESEARCH LABORATORY
CAPTAIN F. R. FURTH, USN, DIRECTOR
WASHINGTON, D.C.

DISTRIBUTION

BuShips	
Attn: Code 841	30
BuAer	
Attn: Code EL-84	5
Attn: Code TD-4	1
Attn: Code EL-71	1
Attn: Code EL 81	1
BuOrd	
Attn: Code Re-4e	5
Attn: Code Re-9e	1
CNO	2
Dir., USNEL	2
Cdr., USNOTS	
Attn: Reports Unit	2
CO, USNUSL, New London	
Attn: Infrared Division	1
BAGR, CD, Wright-Patterson Air Force Base	
Attn: CADO-D13	1
OCSigO	
Attn: Ch. Eng. & Tech. Div., SIGTM-S	1
CO, SCEL	
Attn: Dir. of Engineering	2
CG, AMC, Wright-Patterson Air Force Base	
Attn: Eng. Div., Electronics Subdiv., MCREEO-2	1
CO, Watson Labs., Red Bank	
Attn: Ch. Eng. Div., WLENG	1
CO, Cambridge Field Station, Cambridge	
Attn: ERCAJ-2	1
RDB	
Attn: Library	2
Attn: Navy Secretary	1
Attn: Electronics Committee Infrared Panel	2
Naval Res. Sec., Science Div.	
Attn: Mr. J. H. Heald	2

CONTENTS

ABSTRACT

An investigation of the effect of synchronized time-gating on the signal-to-noise ratio of a very-low-frequency broadband amplifier was undertaken in an effort to improve the performance of the periscope-mounted thermal detector (Passive Bearing Finder). Measurements were made to determine the effect on rms signal-to-noise ratio of time-gating the output of the amplifier in synchronism with a 5-cps sine-wave input. Experimental results are compared with those given by application of theoretically derived formulae. Experiments were also performed to evaluate the effect of synchronized gating on signal-detection threshold where (1) a visual method of signal presentation and (2) the frequency-modulated tone type of signal presentation are used with the above broadband system.

Experimental results agree with the theoretically derived results and indicate that gating can at best improve rms signal-to-noise ratio by the factor 1.4. No improvement at all was noted where visual or aural presentation was used and, in fact, time-gating the aural system caused a marked deterioration in signal-to-noise ratio.

A brief hypothetical discussion indicates that generally similar results would be expected if the amplifying system were narrowband rather than broadband.

PROBLEM STATUS

This is an interim report. Work is continuing.

AUTHORIZATION

NRL Problem 37NO7-09R (BuShips Problem Request NR486-011 dated November 6, 1946)

PASSIVE BEARING FINDER

REPORT NO. 1

EFFECT OF SYNCHRONIZED TIME-GATING ON THE SIGNAL-TO-NOISE RATIO OF A BROADBAND AMPLIFIER

INTRODUCTION

The Passive Bearing Finder is a thermal detector for use on submarines against surface vessels. It consists of a periscope-mounted, watertight, Maksutov optical system, in the focal plane of which are mounted the two halves of a self-compensating thermopile. The spherical mirror of the system is wobbled horizontally so as to throw, first on one half of the thermopile and then on the other, at a 5-cps rate the image of any small target which lies on the optic axis.

The resulting 5-cps voltage generated by the thermopile is amplified electronically and is then presented aurally as the frequency modulation of a local 1000-cps tone. Unfortunately, the electrical noise level of the associated amplifier is so high that it is impossible adequately to observe the Johnson noise from the thermopile. The result is a reduction in the signal-to-noise ratio.

The origin of the dominant amplifier noise depends upon the method of amplification. One method consists of amplifying the 5-cps output of the thermopile directly with a special low-frequency input transformer and R-C-coupled vacuum tube stages.[1] The noise in this amplifier is due to the flicker effect in the first vacuum tube.[2] A second method consists of mechanically chopping the electrical 5-cps output signal from the thermopile at an 80-cps rate, amplifying it, and then synchronously rectifying it.[3] Since the electronic amplification is done at 80 cps, the flicker effect in the first vacuum tube is not too bothersome. The greatest portion of the noise in this case is electrical contact noise from the mechanical chopper, which, like flicker noise, is very rich in low-frequency components.

---

[1] Clark, H. L., "A 5-cps Amplifier for Use with the Passive Bearing Finder," NRL Report H-2895 (Confidential), 12 July 1946.

[2] Clark, H. L., "Flicker Noise in Vacuum Tubes," NRL Report H-2894 (Unclassified), 28 August 1946.

[3] BuShips Instruction Manual for Passive Bearing Finder, Bureau of Ships, NavShips 3670011, NObs-21176 (Confidential).

In either case, the reduction in signal-to-noise ratio results in an intolerable reduction in the nominal operating range of the entire equipment. Some improvement has been realized by narrowing down the bandwidth of the amplifiers, but experience in the field has shown that the build-up and decay times of the amplifier cannot exceed 0.1 second, a fact which places a lower limit on the bandwidth of the amplifiers.

One possible method of improving the signal-to-noise ratio without increasing the response time of the amplifier is to employ at the output of the amplifier a gating circuit synchronized with the 5-cps wobble of the spherical mirror in the optical system. If the gating circuit is adjusted so that it allows passage of the signal plus noise for only that small fraction of a cycle when the signal is a maximum, some improvement in the signal-to-noise ratio should be realized. It is the purpose of this report to present and compare theoretical and experimental results obtained when synchronized gating was employed at the output of a relatively broadband low-frequency amplifier for each of three cases. The first deals with the presentation of the signal by an rms-type of meter, the second with presentation on an oscilloscope screen, and the third with the use of a pair of earphones. The signal in each case was a 5-cps sine wave, and the electrical noise was predominately flicker noise.

PART I. EFFECT OF CHOPPING ON RMS SIGNAL-TO-NOISE RATIO

(a) Equipment and Experimental Procedure

To investigate the effect of synchronized time-gating on rms signal-to-noise ratio, the signal from a 5-cps motor-driven generator was fed through a micro-volter and broadband amplifier to an electronic thermo-voltmeter. A rotary switch was interposed between the broadband amplifier and the electronic voltmeter and synchronized mechanically with the 5-cps generator so that signal was passed only during some fraction, α, of the 5-cps half-cycle. Phasing was so arranged that the positive and negative peaks of the 5-cps signal were centered in the signal-pass interval. A jumper was used to short the rotary chopping switch when it was desired to make measurements without chopping. An oscilloscope, synchronized with the 5-cps generator signal, was used to monitor the input to the electronic voltmeter so that improper operation of the chopper, extraneous noise pickup, and other abnormal conditions could be readily recognized. The block diagram and the apparatus are shown in Figures 1 and 2. Characteristics and circuit diagrams of the components are given in Figures 3 through 6, and Figures 7 through 10 are photographs of components.

The 5-cps generator, d-c driving motor, and rotary switch are mounted together as one unit (Figure 8). Storage batteries (totalling 24 volts) run the d-c motor at 25 rps, and this in turn is connected by belt and pulleys to drive the two-pole generator and the rotary switch at 5 rps. The cylindrical rotary switch makes contact twice per revolution. The brass contacting surfaces are tapered so that contact durations from less than 0.1 to more than 0.4 of the half-cycle period may be had by positioning a movable wiping contact at the appropriate point along the length of the cylinder.

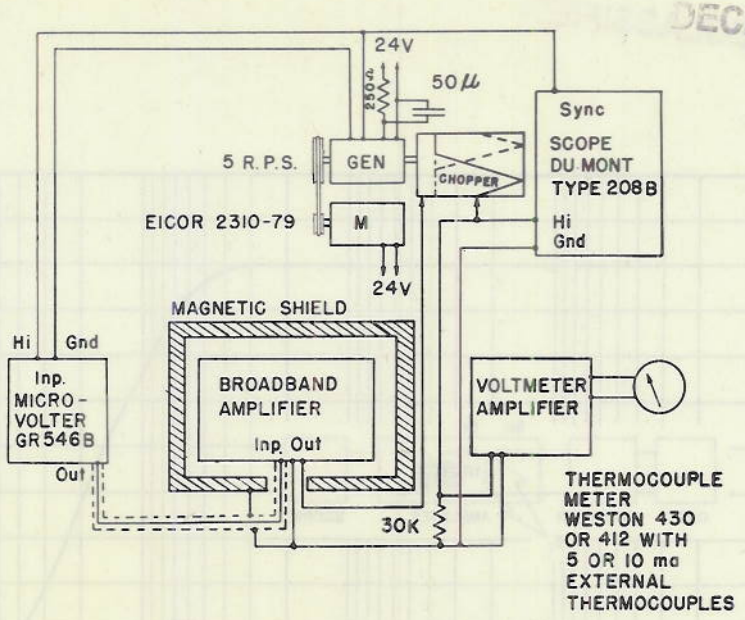

Figure 1 - Block diagram for rms signal-to-noise ratio measurement

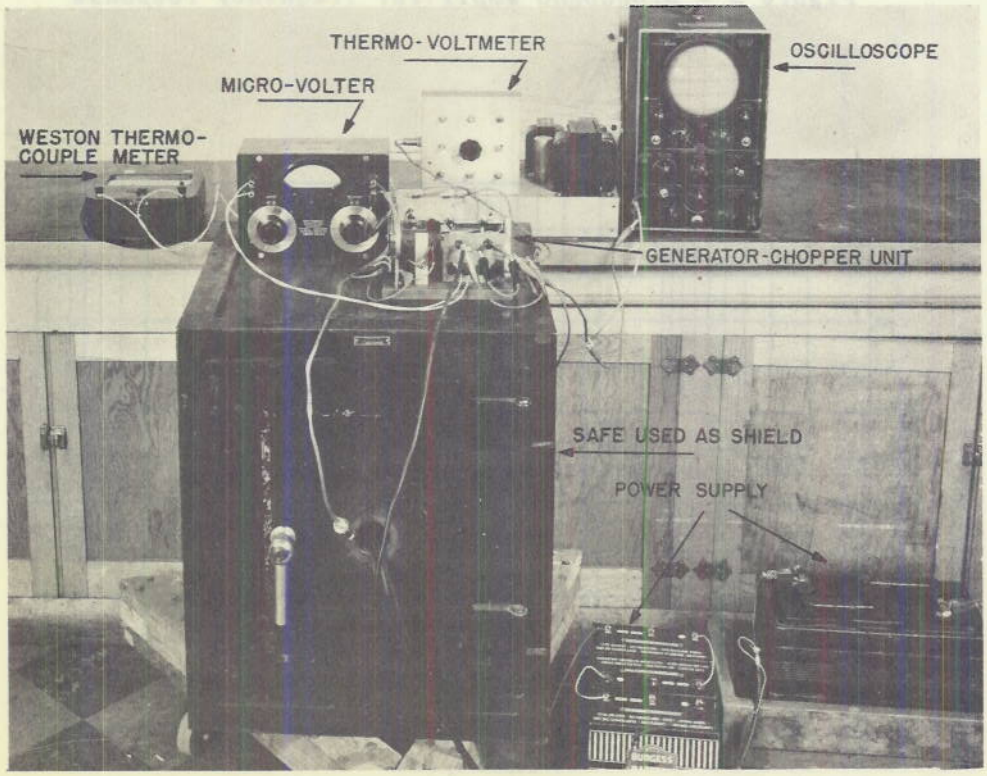

Figure 2 - Assembled equipment for S/N measurement

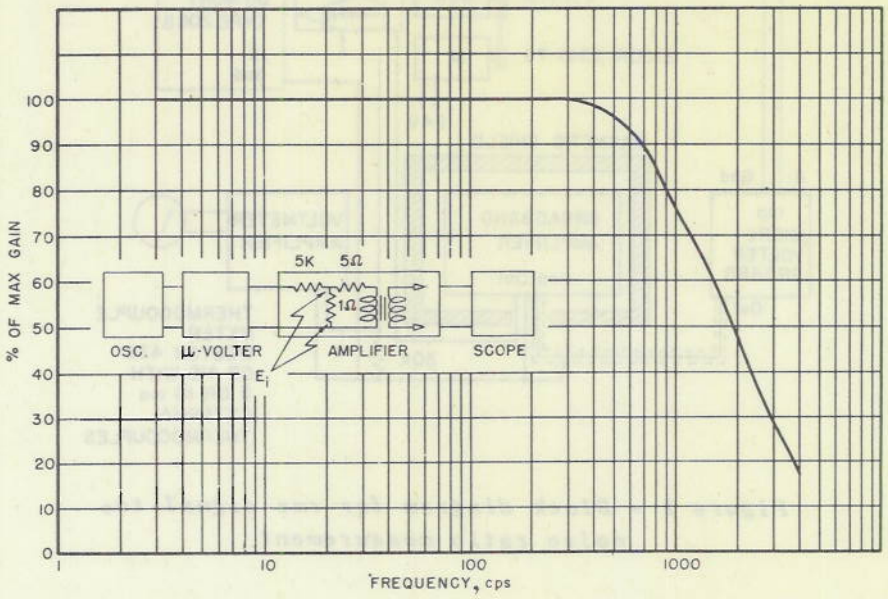

Figure 3 - Broadband amplifier frequency response

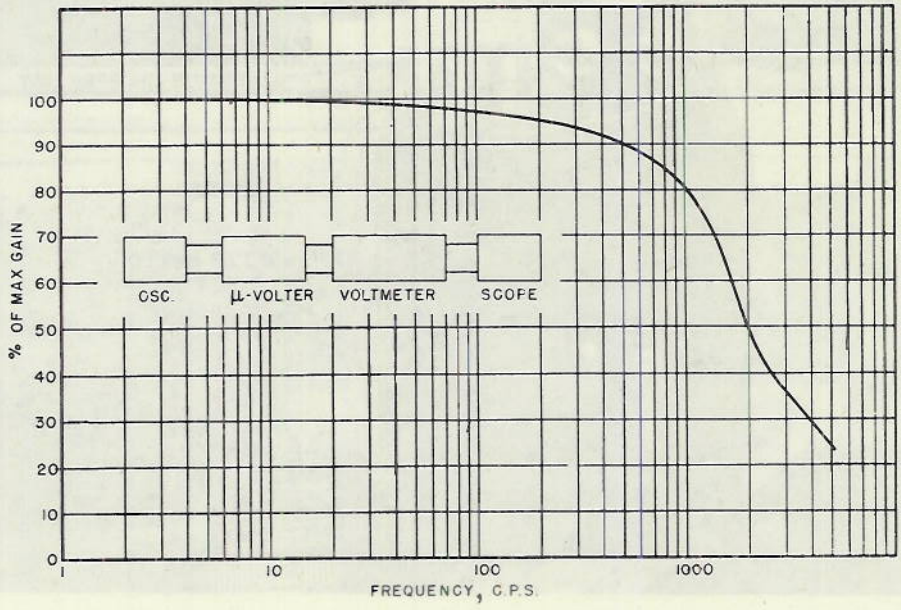

Figure 4 - Voltmeter amplifier response

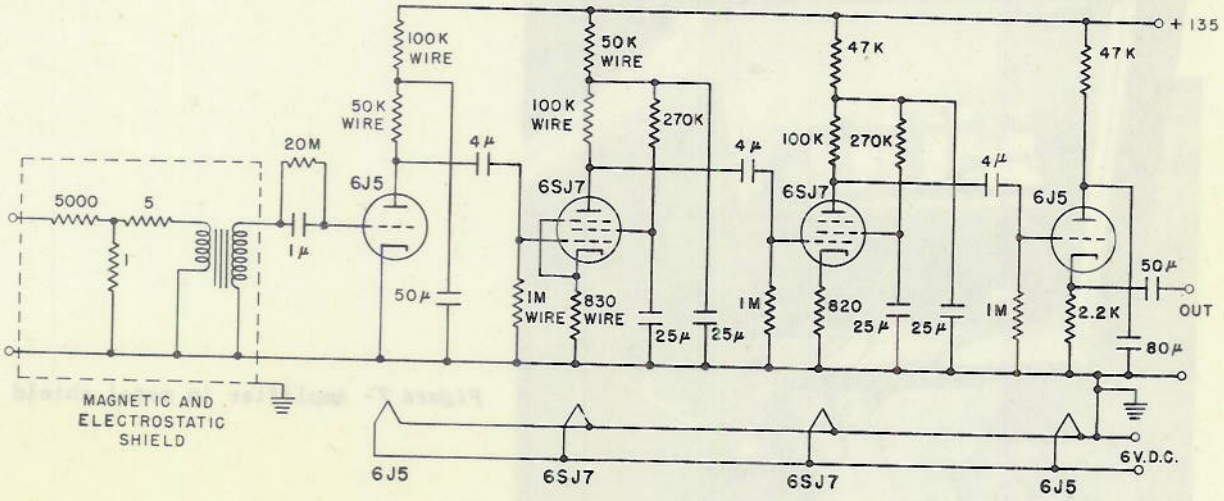

Figure 5- **Broadband amplifier circuit**

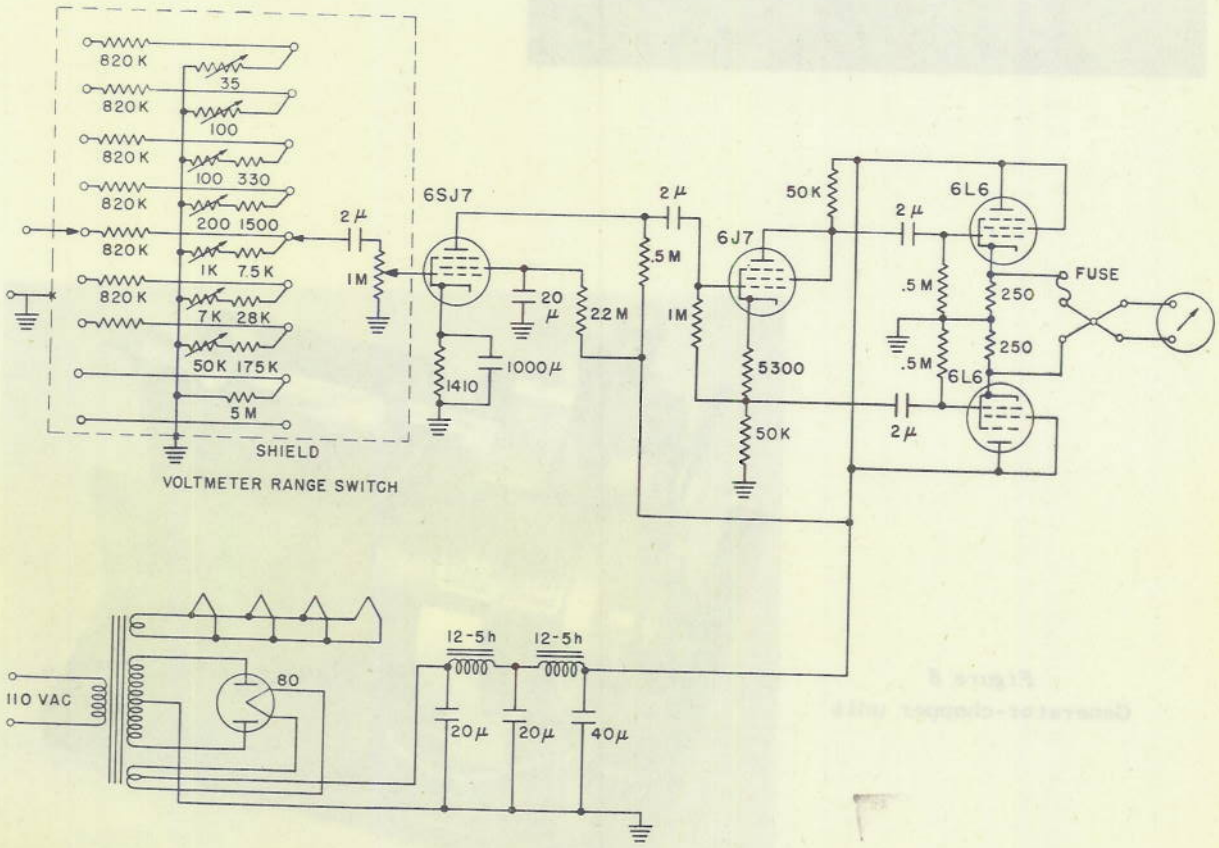

Figure 6- **Electronic voltmeter circuit**

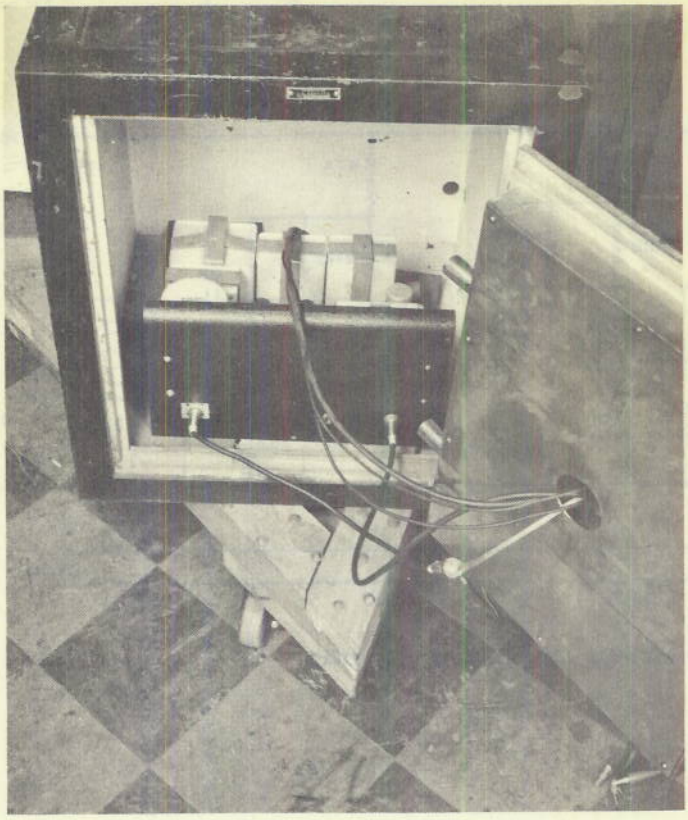

Figure 7- Amplifier in metal shield

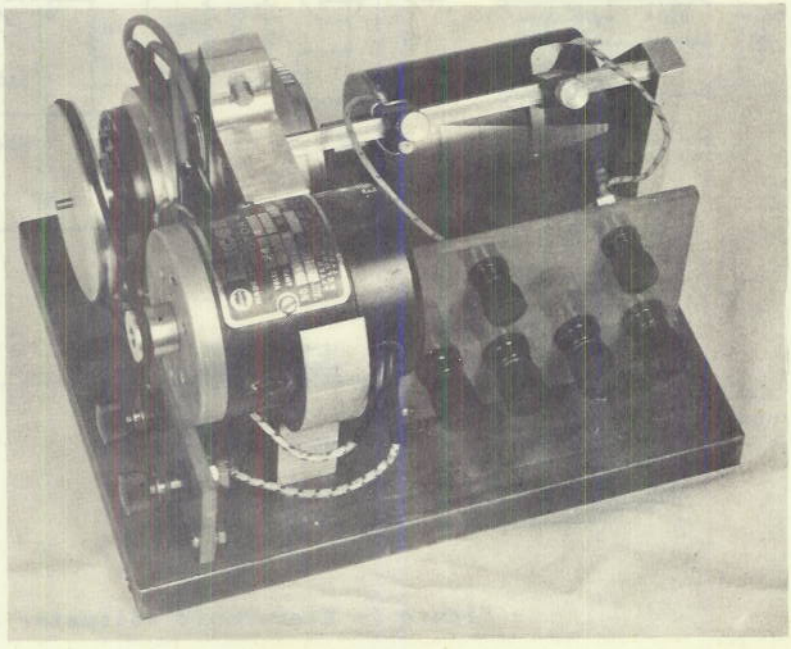

Figure 8
Generator-chopper unit

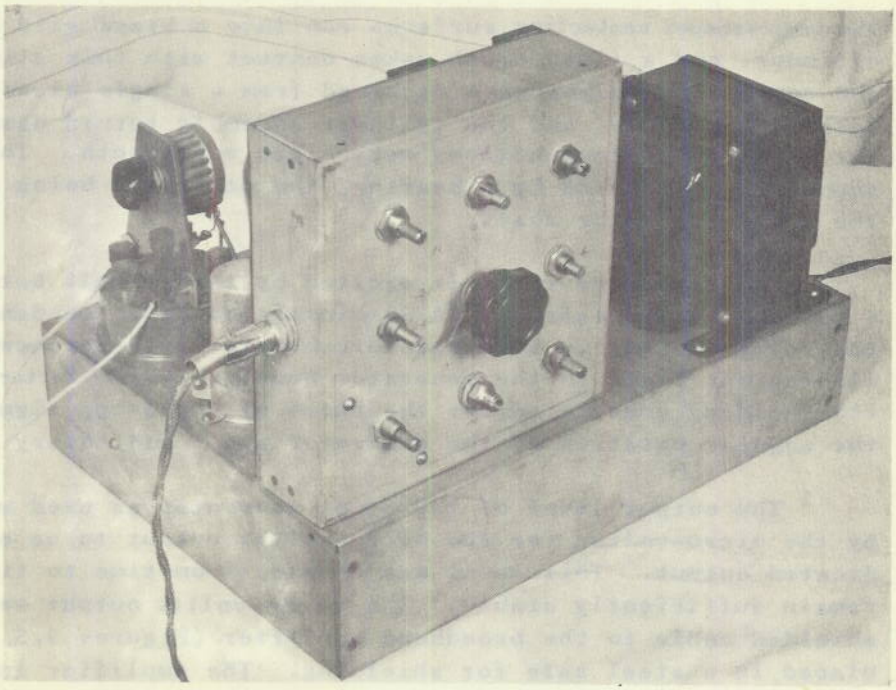

Figure 9 - Electronic thermo-voltmeter, front view

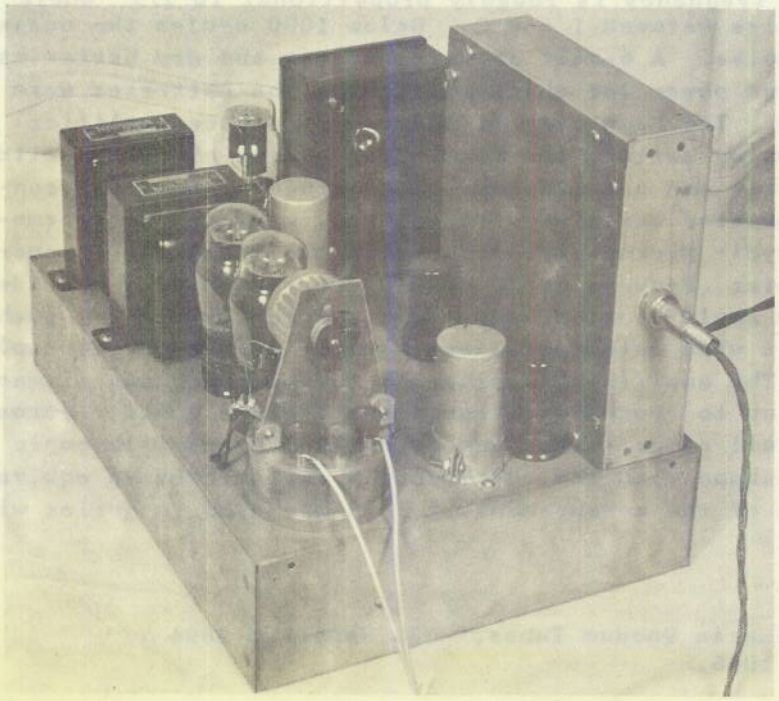

Figure 10 - Electronic thermo-voltmeter, side view

The wedge-shaped contacting surfaces run into a brass slip ring at one end of the cylinder, and a fixed brush makes contact with this slip ring. The slip ring and contacting wedges were machined from a single piece of brass, set in the bakelite cylinder, and the cylinder assembly turned down on a lathe so that the brass-bakelite junctions were flush and smooth. The cylinder shaft is supported at one end by a bearing, the other end being fastened directly to the generator rotor shaft.

The generator rotor is excited by the 24-volt battery source through a 250-ohm field resistor. A 50-microfarad paper condenser was placed across the rotor winding to eliminate brush noise interference. The 5-cps output winding was fixed in the generator housing, which latter could be rotated in its holding yoke to adjust the phase of the 5-cps signal with respect to the angular position of the generator shaft and rotary switch.

The output level of the 5-cps generator as used was just that required by the micro-volter for the micro-volter output to be one-tenth of the indicated output. This level was checked from time to time and was found to remain sufficiently stable. The micro-volter output was fed through a shielded cable to the broadband amplifier (Figures 3, 5, and 7) which was placed in a steel safe for shielding. The amplifier input transformer was a special UTC low-frequency transformer, 2 to 100 cycles, impedances 5 and 500,000 ohms, and was magnetically shielded with several layers of mumetal. The 5000-ohm input attenuator (Figure 5) was built in a mumetal box which fitted over the terminal end of the transformer case so that all low-impedance leads were well shielded magnetically. The circuit of the input stage was one which had been found superior from the standpoint of low flicker and shot noise.[4]

The noise at any frequency is roughly proportional to $1/f^n$ where f is the frequency and n lies between 1 and 2. Below 1000 cycles the noise is predominately flicker noise. A 6-volt storage battery and dry batteries totalling 135 volts supplied power for this amplifier. The batteries were external to the steel safe. The high side of the low-impedance amplifier output was run to the chopping switch, the other side of the chopping switch going to the thermo-voltmeter and oscilloscope. The ground leads were connected directly. A 30K resistor was placed across the input to the thermo-voltmeter to minimize 60-cycle pickup during the open period of the chopper switch. The thermo-voltmeter (Figures 6, 9, and 10) consisted of a shielded range switch, a stage of pentode amplification, and a phase inverter driving push-pull triode-connected 6L6's with cathode follower output to the thermocouple of the indicating meter. The amplifier feeding the thermocouple was linear for output-voltage swings up to roughly fifteen times the rms voltage across the 5-ma thermocouple at full range. This was determined by oscilloscopic observation of output waveshape with the thermocouple replaced by an equivalent resistance. For some of the measurements a fuse was used in series with the thermocouple.

---

[4] Clark, H. L., "Flicker Noise in Vacuum Tubes," NRL Report H-2894 (Unclassified), 28 August 1946..

The general experimental procedure may be outlined as follows, it being assumed that the chopping switch has been set to pass the desired fraction, α, of each cycle of the signal:

1. With no signal input to the amplifier, and with the chopping switch shorted, the noise-voltage output of the amplifier, designated by E_n, was read on the electronic thermo-voltmeter.

2. The micro-volter was advanced to apply the signal from the 5-cps generator to the input of the amplifier and was adjusted so that the output signal-and-noise voltmeter reading, E_{sn}, was $1.41 \times E_n$. It was then assumed that the signal-voltage output, E_s, was equal to the noise voltage output, E_n.

3. The short was removed from the chopping switch, and the chopped signal-and-noise output voltage, E'_{sn}, was read.

4. The micro-volter was retarded to remove the signal from the preamplifier input, and the chopped noise-output voltage, E'_n, was read.

5. The chopping switch was shorted out and E_n again was checked.

For certain of the noise measurements, two additional steps were included:

6. With the chopping switch still shorted out, the amplifier signal input was raised to such a value that noise was negligible in comparison, and the output-signal voltage was read.

7. The short was removed from the chopping switch, and the chopped signal output was read.

(b) Calculation and Presentation of Results

The relationship $E'_s = \sqrt{(E'_{sn})^2 - (E'_n)^2}$ was used to determine E'_s, the chopped signal, and the chopped signal-to-noise ratio, R', was then given by E'_s/E'_n. Since R, the initial or unchopped signal-to-noise ratio, was made unity, the factor of improvement, R'/R, was numerically equal to R'. Measurements were made to determine R'/R for α values of 0.05, 0.1, 0.2, 0.3 and 0.4.

For each value of α, several sets of data were obtained. From the data furnished by procedure steps 1 through 4, values of E'_s/E_s, E'_n/E_n, and R'/R were calculated and are shown as functions of α in Figures 11, 12 and 13. The curves were plotted from theoretically derived values.[5] Points

[5] *See Part I (d), Theoretical Analysis*

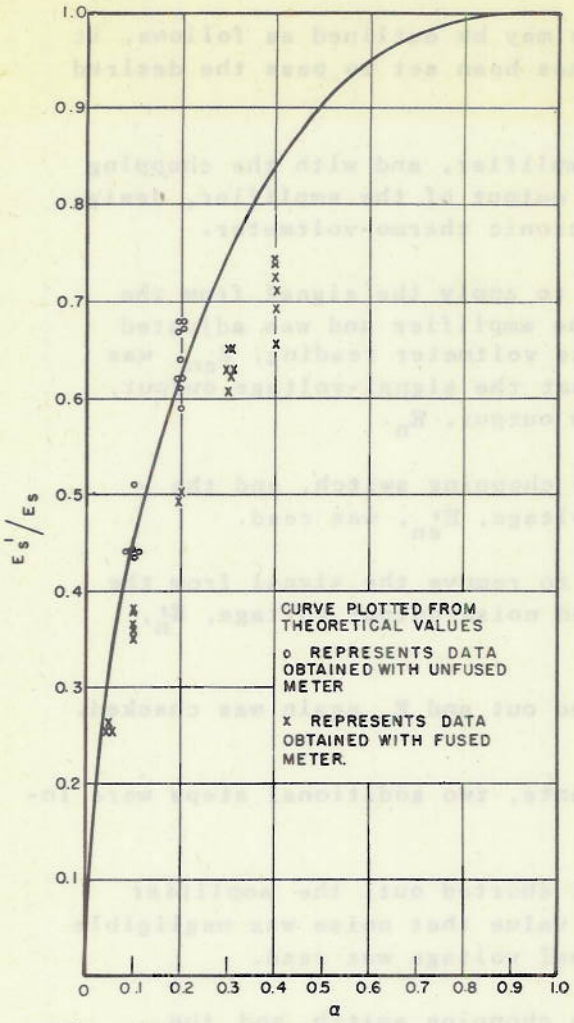

Figure 11-Variation of E_s'/E_s with α

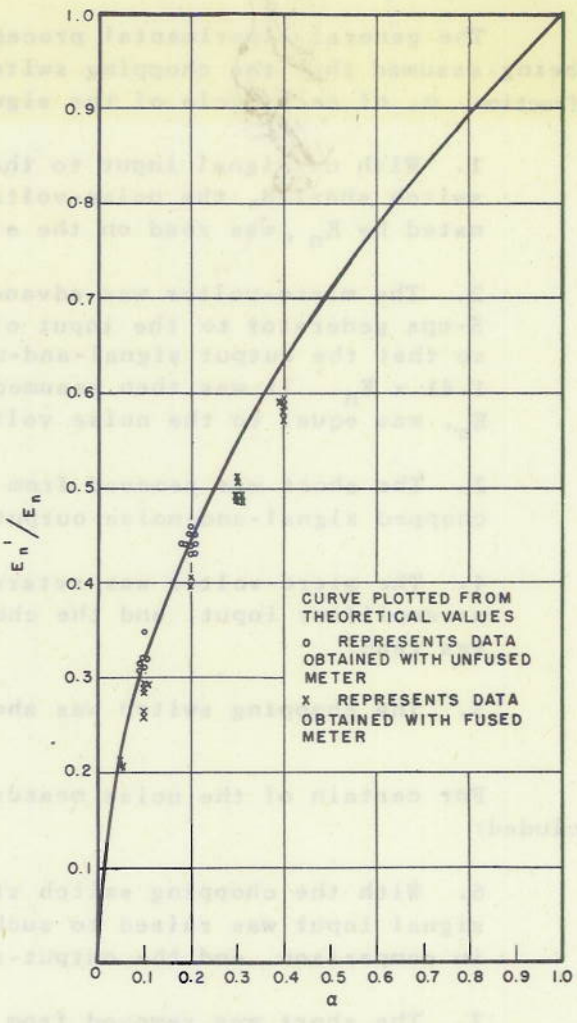

Figure 12-Variation of E_n'/E_n with α

corresponding to data obtained with the unfused meter are plotted with circles, while those corresponding to fused-meter data are plotted with crosses (a discussion of the effect of the meter fuse is given in the next section). From the data obtained when steps 6 and 7 were carried out, where E'_s was measured directly, values of E'_s/E_s were computed. The results are presented graphically in Figure 14 compared with the theoretical values.

The values of E_s'/E_s, E_n'/E_n, and R'/R obtained by steps 1 through 4 without the use of a meter fuse are presented in Figures 15, 16, 17 and 18, again compared with the theoretical values.

(c) Special Experimental Considerations

A few of the more important factors involved in the noise measurements may be noted.

In order that the measured noise would represent tube noise, that is, flicker noise and shot noise, the following precautions were taken:

1. An electrostatically and magnetically shielded matching pad was added to the preamplifier input transformer in such a way that 60-cycle pickup by the low-impedance transformer input leads was made negligible.

2. The broadband low-frequency amplifier was placed in a metal enclosure (a safe) inorder to minimize 60-cycle pickup.

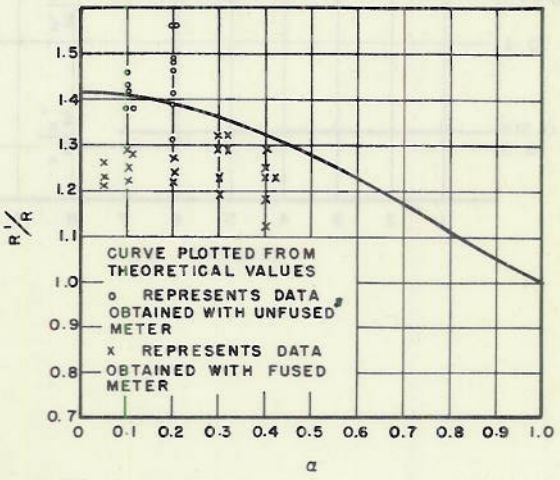

Figure 13- Variation of R'/R with α

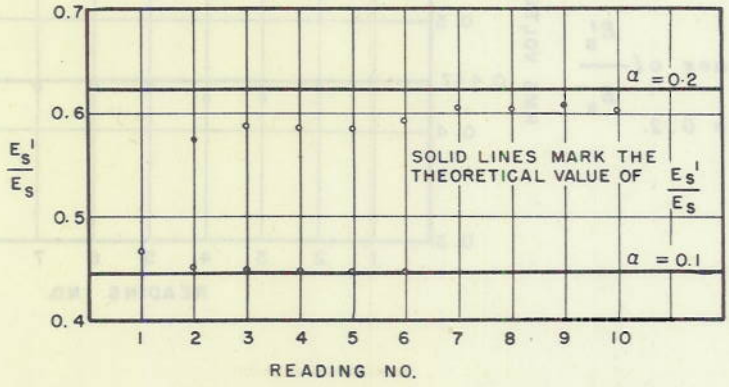

Figure 14-Values E_s'/E_s obtained by direct measurement (procedure steps.6 and 7)

3. Plate and heater batteries were by-passed by 50-mfd paper condensers. Only batteries in good condition were used.

4. A 50-mfd paper condenser was used to by-pass the generator field and eliminate hash interference. With this condenser, operation of the generator had only a very slight effect on the noise level.

5. Care was taken in grounding to avoid paths for circulating currents, and a-c plugs were polarized for minimum 60-cycle pickup.

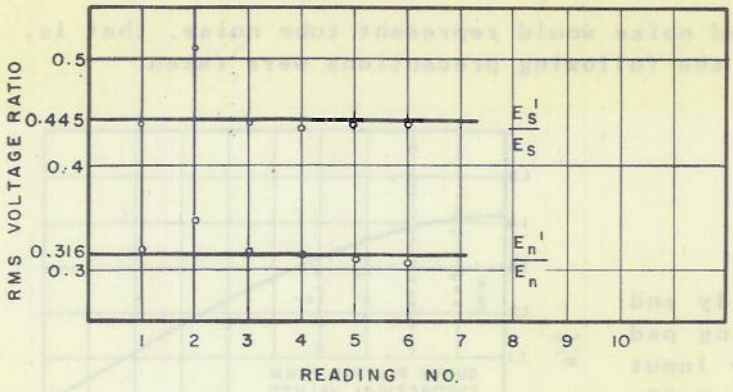

Figure 15 - Values of $\frac{E_s'}{E_s}$ *and* $\frac{E_n'}{E_n}$ *for* $\alpha = 0.1$

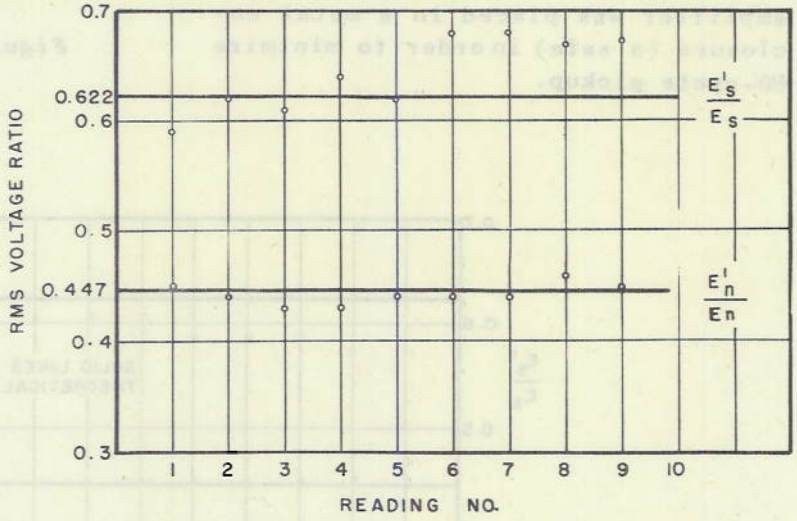

Figure 16 - Values of $\frac{E_s'}{E_s}$ *and* $\frac{E_n'}{E_n}$ *for* $\alpha = 0.2$

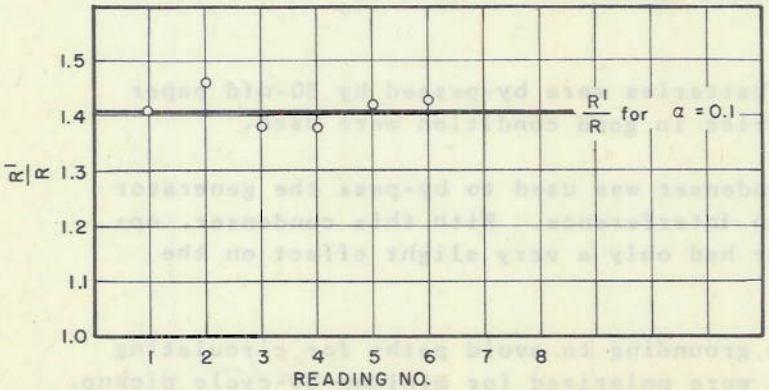

Figure 17 - Values of $\frac{R'}{R}$ *for* $\alpha = 0.1$

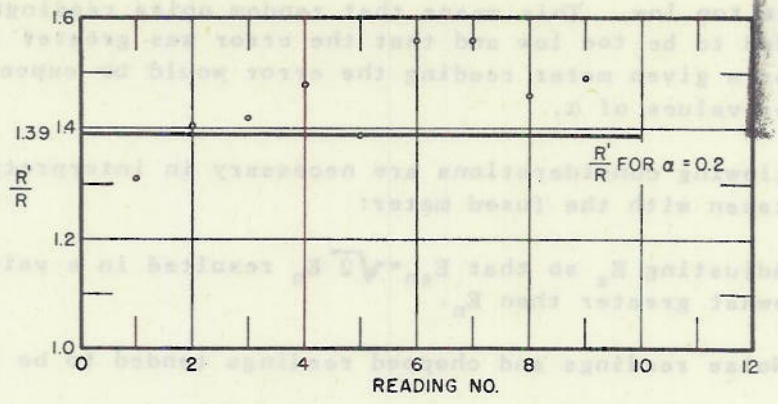

Figure 18 - Values of $\frac{R'}{R}$ for $\alpha = 0.2$

6. Since external signals and transient line-surge effects were not eliminated, measurements were made only under relatively quiet conditions.

7. The signal fed to the voltmeter amplifier was observed on an oscilloscope so that extraneous noise or signal pickup could readily be recognized.

Peak signal level was always kept well below the amplifier overload point and the voltmeter amplifier was designed to be linear for peak swings of ten times the full-scale meter reading.

The micro-volter with standard input was used as a standard for voltmeter calibration. When fed by the 5-cps generator, the output of the micro-volter was very nearly a tenth the indicated value as determined by measurement of the micro-volter output by the voltmeter, the latter previously calibrated by the micro-volter with standard input.

With the thermocouple-type meter, accuracy requires that readings be made with rms current values of at least one fifth of the full meter range. Unfortunately, any overload applied for an appreciable fraction of a second will burn out the thermocouple in a sensitive meter of this type. In attempting to make a series of noise measurements, thermocouple burn-out caused by switching transients and external pickup was so difficult to avoid that it was necessary to use a protective fuse in series with the thermocouple.

For each fuse used, a special meter scale was made using a 20-cps sine-wave calibrating source, and it was determined that the calibration remained valid at 5 cps. However, the very short temperature time constant of the fuse, and the great increase in fuse resistance with current for current values of greater than half-meter range, resulted in considerable errors for wave shapes not approximating a sine wave. In general, when the ratio of peak to effective current was greater than that for a sine wave, meter

readings were too low. This means that random noise readings and all chopped readings tended to be too low and that the error was greater for higher meter readings. For a given meter reading the error would be expected to be greater for smaller values of α.

The following considerations are necessary in interpreting that portion of the data taken with the fused meter:

1. Adjusting E_s so that $E_{sn}=\sqrt{2}\,E_n$ resulted in a value of E_s that is somewhat greater than E_n.

2. Noise readings and chopped readings tended to be too low.

3. The degree of chopped reading error should have been greater for smaller values of α. However, smaller values of α are associated with lower rms meter readings so that this effect was probably masked by the great increase of chopped reading error with rms meter reading.

4. The degree of meter error increased very rapidly with rms meter reading.

(d) Theoretical Analysis of the Effect of Time-Gating on Effective Signal-to-Noise Ratio

It is here assumed that signal and noise will each be measured with a long-time-constant thermocouple meter.

Let E_s be rms signal,
E_n be rms noise,

without time-gating, where the signal is represented by A cos ωt and the noise by f(t), and where f(t) is not functionally related to cos ωt.

$$\text{Now } E_n^2 = \lim_{T\to\infty} \frac{1}{T}\int_0^T \left[\, f(t) \,\right]^2 dt \qquad (1)$$

and

$$E_s^2 = \lim_{T\to\infty} \frac{1}{T}\int_0^T \left[\, A\cos\omega t \,\right]^2 dt = \frac{A^2}{2} \,. \qquad (2)$$

Although T, the sampling interval, is here considered to be infinite, experimentally it represents the time over which the fluctuating meter reading is averaged.

$$\text{Let } R = \frac{E_s}{E_n} \qquad (3)$$

be the signal-to-noise ratio without gating.

Let E'_s, E'_n, and R' be the effective values of signal, noise, and the ratio of them respectively when a gating pulse of duration $\alpha\frac{\pi}{\omega}$ is used (Figure 19), where $o<\alpha<1$.

$$\text{Now } (E'_s)^2 = \lim_{N\to\infty} \frac{\omega}{(N+1)\pi} \sum_{n=o}^{N} \int_{n\frac{\pi}{\omega} - \frac{\alpha\pi}{2\omega}}^{n\frac{\pi}{\omega} + \frac{\alpha\pi}{2\omega}} (A\cos\omega t)^2\, dt \,, \quad (4)$$

$$(E'_n)^2 = \lim_{N\to\infty} \frac{\omega}{(N+1)\pi} \sum_{n=o}^{N} \int_{n\frac{\pi}{\omega} - \frac{\alpha\pi}{2\omega}}^{n\frac{\pi}{\omega} - \frac{\alpha\pi}{2\omega}} [f(t)]^2\, dt \,, \quad (5)$$

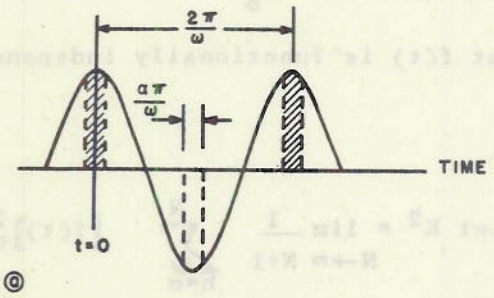

ⓐ

Figure 19 - Time relation between gating pulse and signal

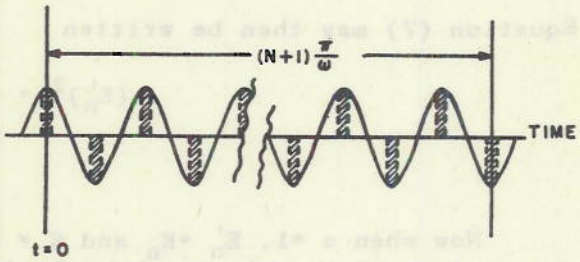

ⓑ

$$\text{and} \int_{n\frac{\pi}{\omega} - \frac{\alpha\pi}{2\omega}}^{n\frac{\pi}{\omega} + \frac{\alpha\pi}{2\omega}} [f(t)]^2 dt = [f(t)]_n^2\, \alpha\frac{\pi}{\omega} \,, \quad (6)$$

where $[f(t)]_n$ is the effective value of $f(t)$ between

$$n\frac{\pi}{\omega} - \frac{\alpha\pi}{2\omega} \quad \text{and} \quad n\frac{\pi}{\omega} + \frac{\alpha\pi}{2\omega} \,.$$

$$\therefore (E'_n)^2 = \alpha\frac{\pi}{\omega} \lim_{N\to\infty} \frac{\omega}{(N+1)\pi} \sum_{n=o}^{N} [f(t)]_n^2 \,. \quad (7)$$

Here, the equivalent sampling time is $(N+1)\frac{\alpha\pi}{\omega}$ or αT, where T is the duration of the observation and (N+1) the number of half-cycles in the observation. In practice, when using chopping, a greater observation time is actually required to secure a good average reading of the meter.

Now when $0 < \alpha < 1$,

$$\lim_{N\to\infty} \frac{1}{N+1} \sum_{n=o}^{N} \left[f(t)\right]_n^2 \quad \text{is a constant and independent of } \alpha.$$

This is true because of the two assumptions that

$$E_n^2 = \lim_{T\to\infty} \frac{1}{T} \int_o^T \left[f(t)\right]^2 dt = \text{a constant}$$

and that f(t) is functionally independent of $\cos\omega t$.

$$\text{Let } K^2 = \lim_{N\to\infty} \frac{1}{N+1} \sum_{n=o}^{N} \left[f(t)\right]_n^2 \quad . \tag{8}$$

Equation (7) may then be written

$$(E_n')^2 = \alpha K^2 \quad . \tag{9}$$

Now when $\alpha = 1$, $E_n' = E_n$ and $K = E_n$. Since K is independent of α, this may be substituted in equation (9) to give: (10)

$$(E_n')^2 = \alpha E_n^2 \quad . \tag{11}$$

By equation (4),

$$(E_s')^2 = \lim_{N\to\infty} \frac{\omega}{(N+1)\pi} \sum_{n=o}^{N} \int_{\frac{n\pi}{\omega} - \frac{\alpha\pi}{2\omega}}^{\frac{n\pi}{\omega} + \frac{\alpha\pi}{2\omega}} \left[A \cos \omega t\right]^2 dt \ ,$$

but

$$\sum_{n=o}^{N} \int_{\frac{n\pi}{\omega}-\frac{a\pi}{2\omega}}^{\frac{n\pi}{\omega}+\frac{a\pi}{2\omega}} [A\cos\omega t]^2\,dt = (N+1)\int_{-\frac{a\pi}{2\omega}}^{\frac{a\pi}{2\omega}} [A\cos\omega t]^2\,dt$$

$$= 2(N+1)\int_{o}^{\frac{a\pi}{2\omega}} [A\cos\omega t]^2\,dt, \qquad (12)$$

So that $(E_s')^2 = \lim_{N\to\infty} \frac{2\omega(N+1)}{\pi(N+1)} \int_{o}^{\frac{a\pi}{2\omega}} [A\cos\omega t]^2\,dt \qquad (13)$

$$= \frac{2\omega}{\pi}\int_{o}^{\frac{a\pi}{2\omega}} [A\cos\omega t]^2\,dt \qquad (14)$$

$$= \frac{A^2}{\pi}\left[\sin\frac{a\pi}{2}\cos\frac{a\pi}{2} + \frac{a\pi}{2}\right]. \qquad (15)$$

But by equation (2), $A^2 = 2E_s^2$, so that

$$(E_s')^2 = \frac{2E_s^2}{\pi}\cdot\left[\sin\frac{a\pi}{2}\cos\frac{a\pi}{2} + \frac{a\pi}{2}\right]. \qquad (16)$$

From equations (11) and (16) we have

$$R' = \frac{E_s'}{E_n'} = \sqrt{\frac{2E_s^2}{\pi}\cdot\frac{1}{aE_n^2}\left[\sin\frac{a\pi}{2}\cos\frac{a\pi}{2} + \frac{a\pi}{2}\right]}, \qquad (17)$$

$$R' = R\sqrt{\frac{2}{a\pi}\left[\sin\frac{a\pi}{2}\cos\frac{a\pi}{2} + \frac{a\pi}{2}\right]}, \qquad (18)$$

and $$\frac{R'}{R} = \sqrt{\frac{\sin a\pi}{a\pi} + 1}\,. \qquad (19)$$

Thus, the range of variation of $\frac{R'}{R}$ is seen to lie between $\sqrt{2}$ and 1.

PART II. EFFECT OF CHOPPING ON VISUAL SIGNAL-DETECTION THRESHOLD

(a) Experimental Procedure and Tabulation of Data

The effect of chopping on visual signal detection was investigated by applying a 5-cps signal through a micro-volter to the broadband amplifier (Figures 3, 5 and 7) and feeding the output of the amplifier through the mechanically synchronized chopper unit (Figure 8) to the vertical plates of an oscilloscope (Figure 20).

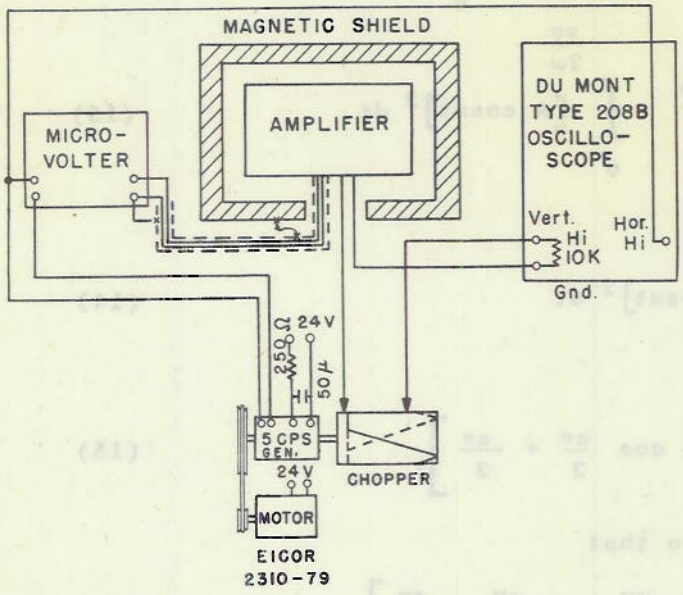

Figure 20 - Block diagram, apparatus for measuring visual signal-detection threshold in presence of noise.

The original 5-cps signal was used for the oscilloscope sweep so that, with chopping, the effect of a signal was to produce pulses of opposite polarity at the extremes of the sweep. Without chopping, the effect of a signal was to incline the sweep with respect to its normal horizontal position. This mechanically synchronized sine-wave sweep was found to be equivalent to the electrically synchronized linear sweep from the standpoint of signal recognition but has the advantage of absolute stability and simplicity of application in a practical system. Typical oscilloscope patterns with the sine-wave sweep are sketched in Figure 21.

The 10K resistor shunting the oscilloscope input did not materially affect the calibration of the micro-volter. This resistor was used to eliminate the hum pickup which otherwise would have been present during the interval the chopping switch was open and which would have been significant in comparison with the no-noise thresholds if a much higher value of shunting resistor had been used.

The oscilloscope gain was adjusted so that amplifier noise gave a convenient deflection, and then the level of the 5-cps signal was adjusted so that its presence could just be detected visually, with and without

(a) NORMAL OPERATION:

Figure 21 - Oscilloscope visual-presentation patterns

(b) CHOPPED OPERATION:

chopping. This minimum perceptible signal, measured at the amplifier input, was multiplied by 600, the gain of the amplifier, to refer it to the oscilloscope input. Measurements of minimum perceptible signal in the presence of noise were made with and without chopping for α values of 0.05, 0.1, 0.2, 0.3, and 0.4, and the results, referred to the oscilloscope input, are given in Table 1. The rms amplifier noise output (unchopped) was approximately 30 mv.

TABLE 1

Visual Signal-Detection Threshold with 30-MV RMS Noise Interference

α	Minimum Detectable Signal	
	Normal MV	Chopped MV
0.05	12.6	11.4
0.05	12.6	11.4
0.1	12.6	12.0
0.1	11.4	10.8
0.2	13.2	8.4
0.2	11.4	9.0
0.3	13.2	11.4
0.3	16.2	8.4
0.4	13.2	11.4
0.4	14.4	12.0

To determine the minimum perceptible signal without noise interference, the micro-volter output was fed directly to the chopper and oscilloscope (Figure 22), and measurements were made with and without chopping for α values of 0.05, 0.1, 0.2, 0.3, and 0.4. The results, given in Table 2, show the noise-free detection threshold of the visual system to be several hundred times lower than the threshold in the presence of 30 mv of noise. It is seen that chopping has no noticeable effect on the noise-free detection threshold and very little effect on the threshold in the presence of noise.

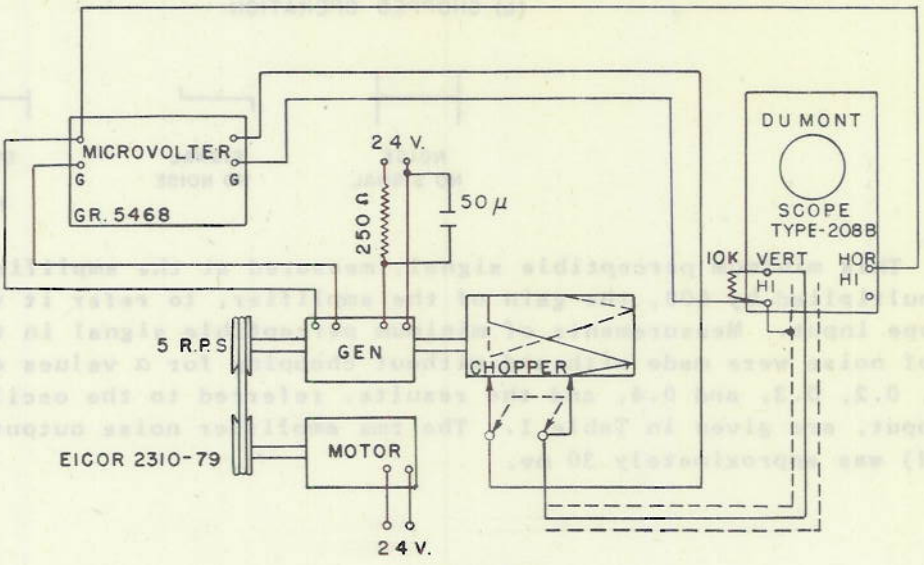

Figure 22 - Block diagram, apparatus for measuring visual signal-detection threshold without noise.

(b) Interpretation of Results

In interpreting the data given in Tables 1 and 2, it must be remembered that the threshold of any sense perception is fuzzy and that individual readings made under the same physical conditions may be expected to vary over quite a range. It appears that chopping has no measurable effect on noise-free minimum signal perception but that there is a slight decrease in the value of the minimum signal that can be perceived in the presence of noise when chopping is used. The results did not appear to be noticeably related to the value of α in the range 0.05 to 0.4. As would be expected, the effect of chopping was to cut out the less significant part of the picture and to replace it with a convenient baseline. Superfluous noise which tended to distract the eye was removed, and pattern dissymetry due to signal was emphasized by the sweep reference line.

TABLE 2

Visual Signal-Detection Threshold without Noise Interference

α	Minimum Detectable Signal	
	Normal MV	Chopped MV
0.05	0.024	0.023
0.05	0.020	0.028
0.1	0.020	0.022
0.1	0.019	0.019
0.2	0.021	0.018
0.2	0.020	0.022
0.3	0.021	0.013
0.3	0.016	0.019
0.4	0.021	0.019
0.4	0.018	0.021

PART III. EFFECT OF CHOPPING ON AURAL SIGNAL-DETECTION THRESHOLD

(a) Experimental Procedure and Tabulation of Data

To evaluate the effect of time-gating on aural signal detection, the signal from the 5-cps generator was fed through the micro-volter, broadband amplifier, and chopper switch to an amplifier-modulator unit. A block diagram of the apparatus is given in Figure 3 . Except for the amplifier-modulator unit, the components are those already described.

The amplifier-modulator unit (Figure 4), contained an audio oscillator frequency-modulated by the incoming signal, and earphones were used to listen to the frequency-modulated tone. A regular 5-cps variation in pitch indicated the presence of an unchopped signal, while pulses of tones alternately higher and lower than the center frequency were characteristic of the effect of a chopped signal. Unchopped noise caused a rough sound in the phones randomly varying over a limited range of average pitch. Signal in the presence of noise (with no chopping) was detected by a regular 5-cps variation in this average pitch. Chopped noise was characterized by a 10-per-second punctuation of the center tone by pulses of rough sound. In this case, the presence of a signal was indicated by a regular alternation, pulse to pulse, in the average pitch of the noise pulses.

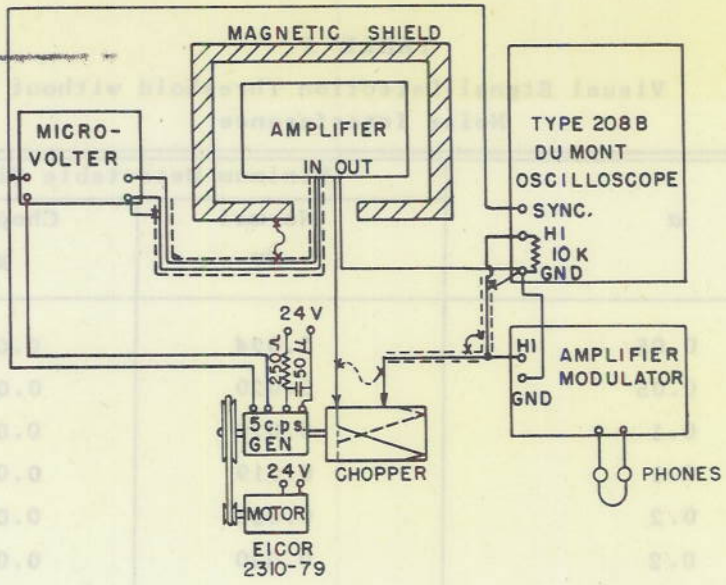

Figure 23 - Block diagram, apparatus for measuring aural signal-detection threshold in presence of noise

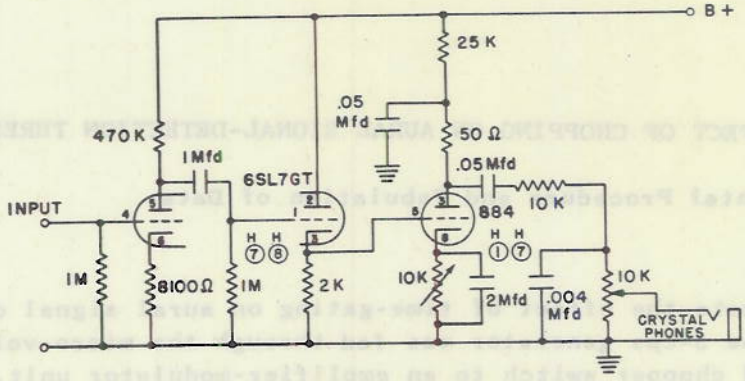

Figure 24 - Amplifier-modulator circuit

The micro-volter reading at which the presence of the signal could just be detected was recorded and divided by 10 to give the true micro-volter output since, when operated from the 5-cps generator, the micro-volter output was 1/10th of the output with standard input. The resulting figure was multiplied by 600 (the amplifier gain) to give the input to the chopper and amplifier-modulator unit. All threshold readings are referred to this point. Readings were made of minimum detectable signal in the presence of 30-rms millivolts of noise without chopping and with chopping for α values of 0.05, 0.1, 0.2, 0.3, and 0.4. Similar readings of minimum detectable signal without noise were made with the micro-volter feeding directly to the chopper

and amplifier-modulator unit. The results of these measurements for a center frequency of 700 cps are given in Tables 3 and 4. The results of another experiment using a center frequency of 1200 cps, are given in Tables 5 and 6. The oscillator wave shapes are sketched for these two center frequencies. The strong harmonic content of the waves seemed to facilitate weak-signal detection.

(b) Interpretation of Results

The data clearly indicate that the effect of chopping is to increase the threshold of signal detection, both in the presence and absence of noise, and that this increase is greater for smaller values of α. This effect was due to the deterioration of aural pitch discrimation for the shorter-duration chops in which the tone of the sound was heavily masked by the transient percussion and the aural effect was a click rather than a tone pulse.

TABLE 3

Aural Signal-Detection Threshold with 700-CPS Center Frequency and with 30-MV RMS Noise Interference

α	Minimum Detectable Signal	
	Normal	Chopped
	MV	MV
0.05	24	78
0.05	24.6	66
0.05	27.3	66
0.1	30	60
0.1	30	42
0.1	30	54.6
0.2	30	60
0.2	24	42
0.2	24	36
0.3	24	30
0.3	27	36
0.3	30	36
0.4	27	33
0.4	24	31.2
0.4	27.6	30

TABLE 4

Aural Signal-Detection Threshold with 700-CPS Center Frequency without Noise Interference

α	Minimum Detectable Signal	
	Normal MV	Chopped MV
0.05	1.6	3.0
0.05	1.4	4.0
0.1	1.2	3.0
0.1	1.2	2.6
0.2	1.0	2.5
0.2	1.0	2.6
0.3	0.9	2.2
0.3	1.0	2.0
0.4	0.8	1.9
0.4	1.0	1.9

700-CPS Wave Shape

TABLE 5

Aural Signal-Detection Threshold with 1200-CPS Center Frequency and with 30-MV RMS Noise Interference

α	Minimum Detectable Signal	
	Normal MV	Chopped MV
0.05	16.8	42.0
0.05	18.0	54.0
0.1	16.2	42.0
0.1	19.2	39.0
0.2	18.6	39.0
0.2	18.6	39.0
0.3	20.4	40.2
0.3	22.8	36.6
0.4	18.0	33.0
0.4	21.6	27.0

TABLE 6

Aural Signal-Detection Threshold with 1200-CPS Center Frequency without Noise Interference

α	Minimum Detectable Signal	
	Normal MV	Chopped MV
0.05	0.7	2.3
0.05	0.7	3.0
0.1	0.8	1.4
0.1	0.8	2.5
0.2	1.4	2.4
0.2	1.5	2.6
0.3	1.5	2.4
0.3	1.3	1.8
0.4	0.6	0.7
0.4	0.6	0.7

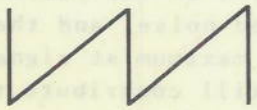

1200-CPS Wave Shape

GENERAL CONCLUSIONS

Time-gating offers the possibility of raising the rms signal-to-noise ratio by the factor 1.4. Where sensitivity is determined solely by the rms signal-to-noise ratio (without regard for wave shape), the over-all sensitivity of the system could be improved proportionately. Unfortunately, the long time constant necessary for such improvement would make a system like the Passive Bearing Finder too sluggish, and thus it cannot here be realized.

When the method of signal presentation is such that time discrimination is automatically provided, as in the visual system, no real increase in sensitivity should be expected.

In the aural system, time-gating might be expected to help matters by providing the ear with a phase reference. Such a phase reference is not needed, however, in the broadband system since detection is based on the rhythmic 5-cps variation in the average pitch of the noise, which latter in practice is caused only by signal. It is not necessary to know the phase of this rhythmic variation since its mere presence indicates a signal. Actually, time-gating causes a deterioration in signal-to-noise ratio by shortening the time available for tonal perception and by introducing the 10-cps pulsing of noise, itself having a masking effect.

Although this report has been concerned with broadband systems, it is believed that the above results may to some extent be used to estimate the effect of time-gating on otherwise similar narrowband systems. The theoretical analysis is not affected by bandwidth, and so the results for rms signal-to-noise ratio should be as found here. Also, the remarks concerning the visual-presentation system should apply regardless of the bandwidth, assuming the observer is trained.

In the case of the aural system, the situation is somewhat different. The narrowband circuits are shock-excited by noise so that noise appears as a succession of 5-cps transients, damped and randomly phased but otherwise similar in character to signal. The long time regularity of the signal distinguishes it from the erratic noise transients, but under threshold conditions this regularity is masked by the noise transients. It would seem that a phase reference would be a real help in differentiating between signal and noise, especially if signal and noise could be heard separately.

Actually, one must listen to the vector addition of the regular signal and the randomly phased noise, and the result is simply an amplitude distribution in phase with a maximum at signal phase. Even so, the phase reference apparently would still contribute to signal-noise discrimination. However, very rough qualitative experiments with a narrowband system indicate that the undesirable effects of time-gating the aural system—the shortened time for pitch discrimination and the masking effect of cutting the noise on and off at a 10-cps rate—more than offset the theoretical advantage of a phase reference.

* * *